SCIENCE CHINA
Earth Sciences

SPECIAL TOPIC: China since the Last Glacial Maximum
•RESEARCH PAPER•

August 2019 Vol.62 No.8: 1288–1301
https://doi.org/10.1007/s11430-018-9240-x

Late Holocene hydroclimatic variations and possible forcing mechanisms over the eastern Central Asia

Jianghu LAN[1], Hai XU[2*], Keke YU[3], Enguo SHENG[4], Kangen ZHOU[1,5], Tianli WANG[1,5], Yuanda YE[1,5], Dongna YAN[1,5], Huixian WU[1,5], Peng CHENG[1], Waili ABULIEZI[6] & Liangcheng TAN[1,7]

[1] *State Key Laboratory of Loess and Quaternary Geology, Institute of Earth Environment, Chinese Academy of Sciences, Xi'an 710061, China;*
[2] *Institute of Surface-Earth System Science, Tianjin University, Tianjin 300072, China;*
[3] *Key Laboratory of Disaster Monitoring and Mechanism Simulating of Shaanxi Province, Baoji University of Arts and Sciences, Baoji 721013, Shaanxi, China;*
[4] *State Key Laboratory of Environmental Geochemistry, Institute of Geochemistry, Chinese Academy of Sciences, Guiyang 550002, China;*
[5] *University of Chinese Academy of Sciences, Beijing 100049, China;*
[6] *Administrative Committee of Lake Sayram, Bozhou 833400, China;*
[7] *Institute of Global Environmental Change, Xi'an Jiaotong University, Xi'an 710049, China*

Received February 13, 2018; revised April 20, 2018; accepted June 25, 2018; published online September 11, 2018

Abstract Hydroclimatic variations over the eastern Central Asia are highly sensitive to changes in hemispheric-scale atmospheric circulation systems. To fully understand the long-term variability and relationship between hydroclimate and atmospheric circulation system, we present a high-resolution lascustrine record of late Holocene hydroclimate from Lake Sayram, Central Tianshan Mountains, China, based on the total organic carbon, total nitrogen, and carbonate contents, carbon/nitrogen ratios, and grain size. Our results reveal four periods of substantially increased precipitation at the interval of 4000–3780, 3590–3210, 2800–2160, and 890–280 cal yr BP, and one period of slightly increased precipitation from 1700–1370 cal yr BP. These wetter periods broadly coincide with those identified in other records from the mid-latitude Westerlies-dominated eastern Central Asia, including the northern Tibetan Plateau. As such, a similar hydroclimatic pattern existed over this entire region during the late Holocene. Based on a close similarity of our record with reconstruction of North Atlantic Oscillation indices and solar irradiance, we propose that decreased solar irradiance and southern migration of the entire circum-North Atlantic circulation system, particularly the main pathway of the mid-latitude Westerlies, significantly influenced hydroclimate in eastern Central Asia during the late Holocene. Finally, the inferred precipitation at Lake Sayram has increased markedly over the past 100 years, although this potential future changes in hydroclimate in Central Asia need for further investigation.

Keywords Lake Sayram, Hydroclimatic variation, Late Holocene, Mid-latitude Westerlies, North Atlantic Oscillation index

Citation: Lan J, Xu H, Yu K, Sheng E, Zhou K, Wang T, Ye Y, Yan D, Wu H, Cheng P, Abuliezi W, Tan L. 2019. Late Holocene hydroclimatic variations and possible forcing mechanisms over the eastern Central Asia. Science China Earth Sciences, 62: 1288–1301, https://doi.org/10.1007/s11430-018-9240-x

1. Introduction

Climate change and associated hydroclimatic variations can have important effects on the environment, ecology, and society (Hodell et al., 1995; Zhang et al., 2008; Liu Y et al., 2009; Buckley et al., 2010; Pederson et al., 2014; Tan et al., 2015; Putnam et al., 2016). Due to the sparseness and short length of available instrumental records, detailing the nature

* Corresponding author (email: xuhai@tju.edu.cn)

of climate changes and its driving mechanisms during the late Holocene is essential for understanding both the regional and global climate dynamics. Moreover, it is important for accurately evaluating future climate trends in the context of anthropogenic climatic warming.

Some studies have investigated climate change during the Medieval Warm Period (MWP), Little Ice Age (LIA), and over much longer time scales, which have largely improved our understanding of past climate change and possible future trends (e.g., Diaz et al., 2011; Graham et al., 2011). For example, Tan et al. (2015) used speleothem oxygen isotope data to infer that drought events interrupting otherwise wet intervals caused major societal disruption, and argued that future precipitation in Central China may be lower than the average of the past 500 years. Cook et al. (2004) reported that the western United States experienced elevated aridity during the MWP, and proposed that any trend of toward warmer temperatures in the future could lead to a serious long-term aridity increase over that region.

However, the forcing mechanisms of climate variability over the late Holocene remain debated. Solar variability can directly force the changes in temperature (Gray et al., 2010; Swingedouw et al., 2011), and indirectly drive the climate changes by influencing ocean-atmosphere interactions (Bond et al., 2001; Zhang et al., 2008; Moffa-Sánchez et al., 2014). For example, decreased solar irradiance during the LIA promoted the development of a quasi-stationary high-pressure system over the eastern North Atlantic region, which further modified the regional atmospheric circulation pattern and contributed to the consecutive cold winter in Europe (Moffa-Sánchez et al., 2014). Moreover, the sea-ice extent in high-latitude oceans (Sha et al., 2014, 2016), surface sea temperature and atmospheric circulation over the North Atlantic Ocean (Wirth et al., 2013; Moffa-Sánchez et al., 2014; Thiéblemont et al., 2015; Orme et al., 2017) and tropical Pacific Ocean (Yan et al., 2011, 2015), and century-scale variability in Yucatan droughts (Hodell et al., 2001) have all been explained by solar forcing. Nevertheless, model simulations have found that volcanic eruptions and changes in greenhouse gas concentrations have primarily influenced Northern Hemisphere climate over the past millennium, whereas solar forcing probably has had a limited effect (Schurer et al., 2014). Furthermore, Greenland and Antarctic ice cores have revealed that the interannual-to-decadal temperature variability in the Northern Hemisphere during the past 2500 years is driven primarily by the large volcanic eruptions in the tropics and at high latitudes (Sigl et al., 2015).

Eastern Central Asia, with its deserts and adjacent Tianshan, Pamir, and Altai mountain ranges, is located at the confluence between the influences of the mid-latitude Westerlies, Siberian Anticyclone and, in part, Asian Monsoon system. As such, this region is highly sensitive to climate changes (Yang et al., 2009; Huang et al., 2014), and may provide information about hemispheric-scale climatic teleconnections (Lauterbach et al., 2014). Various types of archives have been investigated to document precipitation/moisture variations in Central Asia (Herzschuh, 2006; Chen et al., 2008, 2010; Li et al., 2011; Cheng et al., 2012; Long et al., 2017; Wolff et al., 2017), and it has been proposed that hydroclimatic variability in Central Asia is generally out-of-phase with the East Asian Monsoon region (Chen et al., 2010, 2015; Lan et al., 2018; Li et al., 2017). To completely understand the mechanisms and influences of climate changes during the late Holocene and, in particular, the influence of solar variability and atmospheric circulation change over the Norther Atlantic Ocean on Central Asia, further paleo-hydroclimatic studies are required on different archives with robust age models.

The Tianshan Mountains are informally termed the "water tower of Central Asia" (Chen Y N et al., 2016) and are the source of most large rivers in Central Asia (e.g., the Tarim, Ili, Manas, and Syr-Darya rivers). Due to the fragile ecological environment, the consequences of future global warming at the high altitudes are expected to be more severe than in other regions (IPCC, 2007; Lauterbach et al., 2014). Therefore, the Tianshan Mountains are an important research focus for paleoclimate studies (Jiang et al., 2013; Huang et al., 2014; Liu W et al., 2014; Lan et al., 2018; Wolff et al., 2017).

The aim of this study was to advance our understanding of late Holocene hydroclimatic variability in eastern Central Asia, and the relative forcing roles of solar variability and North Atlantic atmospheric circulation. We investigated a sediment core from Lake Sayram, Central Tianshan Mountains, China, which was analyzed for total organic carbon (TOC), total nitrogen (TN) and carbonate contents, the carbon/nitrogen (C/N), and grain size. These data are used to reconstruct regional hydroclimatic variations, and shed light on the climatic teleconnections between solar variability and North Atlantic Oscillation (NAO) via mid-latitude Westerlies.

2. Study site

Lake Sayram is located in the Central Tianshan Mountains (44°30′–44°42′N, 81°05′–81°15′E, 2074 m above sea level; Figure 1) and was formed in the Pliocene to early Pleistocene. The lake is a hydrologically closed terminal alpine lake surrounded by the Kusunmuqieke, Keguqin, Shaliqieke, and Hanziga mountains, and is 30 km long, 27 km wide, rhombic shaped, ~453 km^2 in surface extent, and has a catchment of ~1408 km^2 (Wang and Dou, 1998; Hu, 2004). The lake water volume is ~261×10^8 m^3 and the mean and maximum lake depths are 56 and 110 m, respectively (in AD2016). The lake is an oligotrophic, cold-water lake with a salinity of 2.78 g L^{-1} and pH of 9.17 in AD2011 (Wu et al., 2012; Liu W

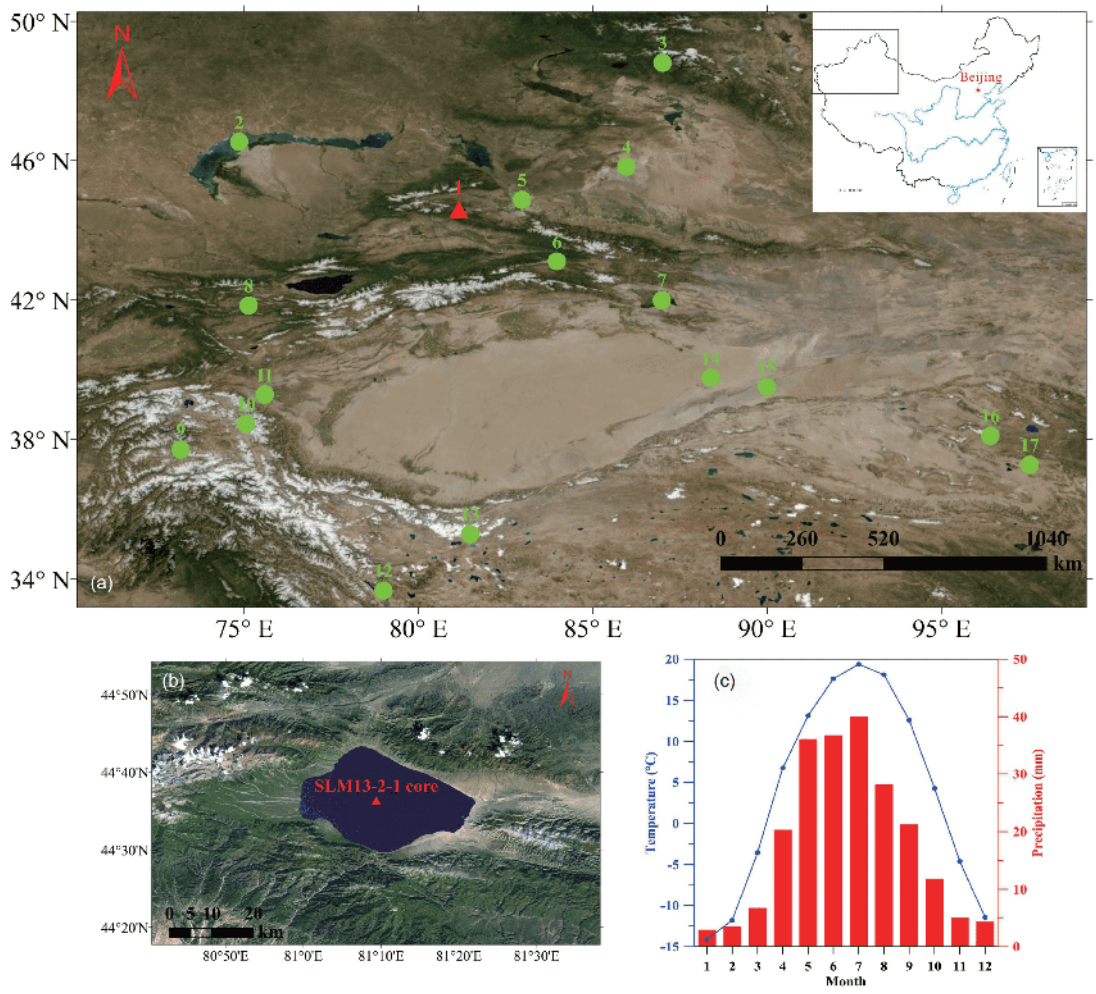

Figure 1 Overview of the study site. (a) Location of the present study area and other sites mentioned in the text throughout eastern Central Asia. Sites 1-17 denote Lake Sayram (this study), Lake Balkhash (Feng et al., 2013), Lake Tiewaike (Li et al., 2017), Lake Manas (Rhodes et al., 1996; Song et al., 2015), Lake Ebinur (Ma et al., 2011; Wang W et al., 2013), Lake Harnur (Lan et al., 2018), Lake Bosten (Chen F H et al., 2006; Mischke and Wunnemann, 2006), Lake Son Kol (Lauterbach et al., 2014), Lake Sasikul (Lei et al., 2014), Lake Kalakuli (Liu X Q et al., 2014; Aichner et al., 2015), Wuper section in Kashgar (Zhao et al., 2012), Lake Bangong (Fontes et al., 1996), the Guliya ice core (Yao et al., 1996; Thompson et al., 1997), a section of aeolian sediment at the eastern margin of the Tarim Basin (Liu et al., 2011), Lop Nor (Putnam et al., 2016), the Dunde ice core (Liu et al., 1998), and the site of a tree ring study in the Qaidam Basin (Wang W Z et al., 2013), respectively. (b) Location of the sampling site at Lake Sayram (SLM13-2-1 core). (c) Mean monthly temperature (blue dotted line) and precipitation (red bars) at Wenquan meteorological station (data from AD1958 to 2016).

et al., 2014). Our measured lake water data by YSI-6600 Z2 show that the lake level has generally increased in recent years, but the hydrological characteristics of the lake water have not changed, which is consistent with the study results of Wu et al. (2012).

Lake Sayram, located in the Eurasian temperate continental high-alpine climate conditions, is characterized by short temperate summers and severely cold winters with ice cover usually from December to early May and an ice thickness of 0.7–1.05 m (Wang and Dou, 1998). The long-term mean annual air temperature, recorded at Wenquan meteorological station (northern of Lake Sayram; Figure 1c), is ca. 3.9°C, with January and July (coldest and warmest months) means of ca. −14.1°C and 19.4°C, respectively (Figure 1c). The mean annual precipitation and evaporation were ca. 236 and 550 mm for the period from AD1958–2016, with a maximum in summer and minimum in winter (Figure 1c). Most of the precipitation is convective rainfall during summer, driven by moist mid-latitude Westerlies air masses (Aizen et al., 2001), and <10 % of the precipitation falls between November and March because of the blocking of the mid-latitude Westerlies by the Siberian Anticyclone in winter.

The lake is supplied mainly by several rivers from the west and northwest, which are fed by rainfall, groundwater, and melting snow from neighboring mountains in its catchment. There are 32 streams around the lake, of which 7 streams are perennial and the others are seasonal (Hu, 2004). The longest river flowing into Lake Sayram is Sagakele River, which is fed mainly by precipitation, is 18 km long and has an average

annual stream flows of 0.240×10^8 m^3. The other streams flow into the lake as surface runoff and/or groundwater, with a combined discharge of 0.699×10^8 m^3. The annual precipitation onto the lake is ca. 1.586×10^8 m^3. In total, the annual water flux to Lake Sayram is ca. 2.525×10^8 m^3. Thus, the lake water is in equilibrium when lake evaporation (~2.492×10^8 m^3; Wang and Dou, 1998) is taken into account. Furthermore, given that the glacier extent in the lake catchment is currently limited (4.28 km^2; Hu, 2004), meltwater has a negligible impact on changes on runoff, lake level, and lake area.

3. Materials and methods

3.1 Fieldwork and sampling

In August 2013, a 121-cm-depth surface sediment core (SLM13-2-1 core) was retrieved from the center of Lake Sayram at a water depth of 83 m, using a 60-mm UWITEC gravity corer (100% sediment recovery; Figure 1b). The upper 10.5 cm of the core is light yellow in color, and the remaining sediments are black, but these are interbedded with 10.5-cm-thick gray-colored sediment units (Figure 2c). The core lithology is fine- to medium-grained silt. The core was sub-sampled *in situ* at 0.5 cm intervals in the upper 50 cm of the core, and at 1 cm intervals for the remainder of the core. Wet samples were kept at 4°C until they were freeze-dried, which is the preferred means for preparing sediment samples, because either air- or oven-drying may result in loss of labile organic matter.

3.2 Dating

To establish a reliable age model, the chronology of the SLM13-2-1 core was determined by Caesium-137 (^{137}Cs) and Lead-210 (^{210}Pb) analysis, and accelerator mass spectrometry radiocarbon (AMS ^{14}C) dating. Radioactivities of ^{137}Cs and ^{210}Pb in the surface sediments were measured by multi-channel gamma spectrometry using an Ortec Germanium (HPGe) well detector (GWL-250-15) at the Institute of Earth Environment, Chinese Academy of Sciences (IEECAS), Xi'an, China. ^{137}Cs and ^{210}Pb activities was measured at 661.6 and 46.5 keV, respectively, with experimental errors of <10% and a detection limits of 0.1 Bg kg^{-1} at the 99% confidence level. The excess ^{210}Pb activity (^{210}Pb$_{ex}$) was calculated by subtraction of the supported activity, which can be approximated as a relatively constant value of ^{210}Pb activity, from the total activity at each level (Xu et al., 2006a). Lake sediments dates determined from ^{210}Pb$_{ex}$ were calculated from the constant rate of supply (CRS) and the constant initial concentration (CIC) models (Appleby et al., 1979). To further constrain the core chronology, 10 samples of bulk organic matter collected from the sediments, owing to without suitable terrestrial residues (Jiang et al., 2013), were dated by AMS^{14}C thechniques after the removal of the carbonates (treatment with diluted HCl) at the Xi'an AMS Center, IEECAS. Due to the anomalously large ^{14}C reservoir age in the saline lakes of northwestern China (Hou et al., 2012; Liu X Q et al., 2014; Yu et al., 2014; Lan et al., 2018), we also evaluated the possible radiocarbon reservoir effect by determining the ^{14}C age of the surface lake sediment around the ^{137}Cs fallout peak.

3.3 Measurement of proxy indices

Bulk carbonate contents (carb%) of sediment samples were determined by titration with diluted perchloric acid ($HClO_4$; 0.1 mol L^{-1}), with an analytical precision of better than 0.5%. The remaining sediments were repeatedly rinsed to neutral pH in distilled water to remove chlorides, and then the TOC and TN contents, and C/N ratios were measured with an elemental analyzer (Vario EL III). Analytical precisions of TOC and TN content are better than 0.1%. For grain size analysis, samples were pretreated with 10% hydrogen peroxide (H_2O_2) and 30% hydrochloric acid (HCl) to remove the organic matter and carbonates, respectively, and then the grain size was determined using a Malvern Mastersizer 2000 laser particle size analyzer. The grain sizes were measured over a size range of 0.02 to 2000 μm, with an error of <3% (Sun et al., 2011, 2015). All these measurements were performed at the IEECAS.

4. Results

4.1 Chronology

4.1.1 ^{137}Cs and ^{210}Pb dating

^{137}Cs is an artificial radionuclide with a half-life of 30.17 year. Atmospheric ^{137}Cs fallout can be detected due to the thermonuclear weapon tests since at AD1945, particularly the multi-national above ground nuclear tests during the early 1950s. The concentration of ^{137}Cs rapidly increased as a result of these tests, and reached its globally maximum value in AD1963 in the Northern Hemisphere (Pennington et al., 1973; Robbins and Edgington, 1975; Wan, 1995). Given that ^{137}Cs would be deposited from the atmosphere within one year, we assigned the ^{137}Cs peak in the lake sediments to be a time marker of AD1964 (Lan et al., 2018; Yu et al., 2017).

^{137}Cs activities in the SLM13-2-1 core show a typical unimodal pattern (Figure 2a) that is similar to the global atmospheric ^{137}Cs pattern (Xu et al., 2010) and thus suggests that the ^{137}Cs peak can be used as a reliable time marker. Therefore, we assigned the ^{137}Cs peak of ca. 180 Bq kg^{-1} at the mass depth of 0.54 g cm^{-2} or the line depth of 2.5 cm in the SLM13-2-1 core to be the 1964-time marker (Figure 2a), and derived a mass accumulation rate of 0.0108 g cm^{-2} yr^{-1}.

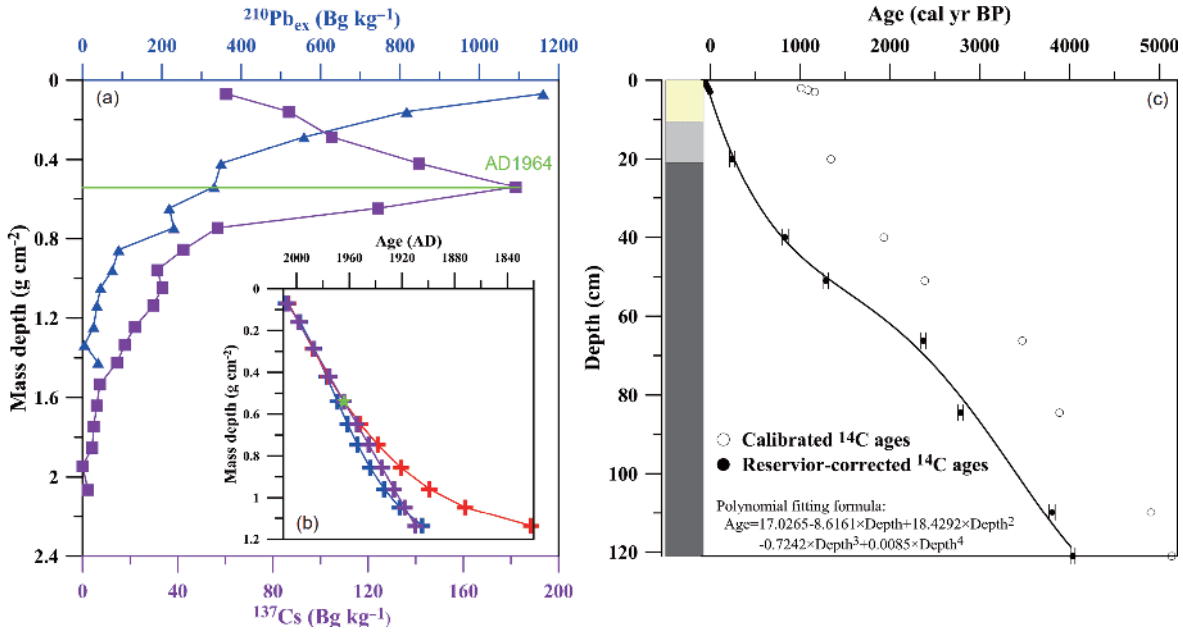

Figure 2 Age model for the Lake Sayram SLM13-2-1 sediment core. (a) Surface sediments ^{137}Cs (purple) and $^{210}Pb_{ex}$ (blue) activities. (b) Age models for the surface sediments. The green star denotes the age of the ^{137}Cs fallout peak. The age models are based on ^{137}Cs activity (purple), and on constant rate of supply (red) and constant initial concentration (blue) of $^{210}Pb_{ex}$. (c) Age model for the core.

This is similar to the rate determined from the $^{210}Pb_{ex}$ age model (0.0109 g cm^{-2} yr^{-1}; see below for the details; Figure 2b). Therefore, the well-defined ^{137}Cs peak most likely corresponds to 1964-time marker rather than the Chernobyl accident in 1986 (Wieland et al., 1993; Putyrskaya et al., 2009; Klaminder et al., 2012; Lei et al., 2014), even though Lake Sayram is relatively close to the Chernobyl.

^{210}Pb is a natural radioactive nuclide in the Uranium-series decay chain with a half-life of 22.23 year, and has been widely used to establish dates of undisturbed sediment cores during the last 100–150 yr (Appleby et al., 1979; Appleby, 2001; Sanchez-Cabeza and Ruiz-Fernández, 2012). Figure 2a shows that the $^{210}Pb_{ex}$ activities at Lake Sayram have a logarithmic decrease down-core. The ^{210}Pb-based chronologies obtained from the CRS and CIC models are generally consistent with each other since AD1964, and also with that of the ^{137}Cs-based chronologies (Figure 2b). For example, at the mass depth of 0.54 g cm^{-2} (2.5 cm), the ^{210}Pb ages produced by the CRS and CIC models are 1963.9 and AD1968.8, respectively, both of which are concordant with the ^{137}Cs age (AD1964). The mean mass accumulation rates calculated by the CRS and CIC models since AD1964 are 0.0109 and 0.0125 g cm^{-2} yr^{-1}, respectively. However, there are discrepancies ages amongst the three dating methods before AD1964, which may be related to the changes in sedimentation rates. Thus, the age model for the surface sediments is established based on the mass accumulation rate inferred from ^{137}Cs-^{210}Pb ages since AD1964.

4.1.2 *^{14}C age model*

The 10 original AMS^{14}C ages were calibrated to calendar years before present (cal yr BP) with the program CALIB 7.0.2 using the INTCAL 09 calibration data set (Stuiver and Reimer, 1993; Reimer et al., 2009). The dating results of SLM13-2-1 core show that the 10 radiocarbon ages present a generally linear correlation with depth. To evaluate possible radiocarbon reservoir effect and systematic measurement errors, we determined the ^{14}C ages for the three uppermost sediment samples, close to the ^{137}Cs fallout peak (AD1964). As shown in Table 1, the results suggest that the average calibrated ^{14}C ages of the three samples at the ^{137}Cs fallout peak are ca. 1087 years (Table 1), which implies that the ^{14}C age is in excess of the ^{137}Cs age by ca. 1073 yr. A possible explanation for this is that the ages determined from bulk organic carbon are affected by the radiocarbon reservoir effect, which is a common problem in the radiocarbon dating of lacustrine sediments in western China. For example, Lake Bosten (Chen F H et al., 2006), Lake Harnur (Lan et al., 2018), Lake Kalakuli (Liu X Q et al., 2014), Lake Gaotai (Yu et al., 2014), and Lake Kusai (Liu X Q et al., 2009) have radiocarbon reservoir effects of 1140, 3560, 1880, 11000, and 3400 yr, respectively.

Based on ^{137}Cs dating results, AD1950 is approximately at the mass depth of lower 0.54 g cm^{-2} (Figure 2b), where an age of 920 yr BP was inferred from the extrapolation of the two uppermost ^{14}C ages. As such, the two independent reservoir-corrected methods yield similar results, which implies that the correction for the radiocarbon reservoir effect

Table 1 AMS^{14}C dating results for bulk sediment samples from Lake Sayram

Lab ID	Sample No.	Depth (cm)	Mass depth (g cm^{-2})	Uncalibrated ^{14}C age ± error (yr BP)	Calibrated age, 1 ó median probability (cal yr BP)	Carbon reservoir effect (yr)	^{137}Cs age (AD)	Reservior-corrected calibrated ^{14}C age by 1073 years (cal yr BP)
XA14624	SLML13-2-1-4	2	0.42	1106±25	1010		1975	
XA11869	SLML13-2-1-5	2.5	0.54	1164±24	1090	1073	1964	
XA14625	SLML13-2-1-6	3	0.65	1229±30	1161		1954	
XA12326	SLML13-2-1-40	20	3.95	1456±27	1343			256
XA12327	SLML13-2-1-80	40	8.68	1982±35	1933			846
XA12328	SLML13-2-1-101	51	11.43	2371±27	2389			1302
XA11870	SLML13-2-1-116	66	15.69	3250±27	3473			2386
XA13271	SLML13-2-1-134	84	21.57	3584±28	3887			2800
XA13272	SLML13-2-1-159	110	31.16	4338±32	4906			3819
XA11871	SLML13-2-1-170	121	35.90	4457±26	5136			4049

(1073 yr) at Lake Sayram is robust. To account for the reservoir effect throughout the entire core, we assumed it was constant, and applied a correction of 1073 yr to all all the calibrated ^{14}C ages. The age model of the SLM13-2-1 core was then established by the fitting a fourth-order polynomial to the reservoir-corrected and calibrated AMS^{14}C dates and ^{137}Cs-^{210}Pb ages (Figure 2c).

4.2 Proxy measurements

As shown in Figure 3, TOC contents of the core ranged between ~3.3% and 8.7%, with an average of 5.6%. The results show that TOC contents were relatively low before 2170 cal yr BP, but interrupted by two periods with high TOC content (~3770–3610 and 3180–2830 cal yr BP), and increased until 910 cal yr BP. Between 890 and 280 cal yr BP, TOC contents were generally low with large fluctuations, followed by a period of higher TOC contents between 280 and 20 cal yr BP. TOC contents have unexpectedly decreased over the past 100 yr (Figure 3). TOC contents do not decrease downwards from the surface sediments, which indicates that the labile organic matter has been decomposed in the lake water and that degradation during early diagenesis has only a minor influence on the TOC contents. TN contents and C/N ratios of the lake sediments generally show similar long-term trends to the TOC contents (apart from 890–280 cal yr BP; Figure 3). Moreover, TOC and TN contents, and C/N ratios are broadly positively correlated with carbonate contents.

The carbonate contents (carb%) in the core vary between 29.9% and 48.5%, with an average of 40.4% during the past 4000 years (Figure 3). There is a decreasing trend before ~2750 cal yr BP, followed by an increasing trend until ~1000 cal yr BP, low contents during the 890–280 cal yr BP, and a decreasing trend over the past 100 yr interrupted by a 150-yr-long period of high carbonate contents (Figure 3).

Prior to ~2000 cal yr BP, the sediment grain size of the SLM13-2-1 core was generally fine-grained silt, particularly at 4000–3780, 3590–3210, and 2800–2160 cal yr BP, which are all broadly contemporaneous with periods of lower of TOC, TN, and carbonate contents, and C/N ratios. The sediment is coarser (~20 μm) from 2000 to 1010 cal yr BP, and slightly finer between 1010 and 400 cal yr BP. Sicne 400 cal yr BP, the grain size shows more variation than earlier in the core (Figure 3).

In summary, all the proxy indices in the Lake Sayram sediments show four periods of distinct character at 4000–3780, 3590–3210, 2800–2160, and 890–280 cal yr BP, and one slightly distinct interval at 1700–1370 cal yr BP. Furthermore, all the proxy indices shown a significant decreasing trend over the past 100 yr (Figure 3).

5. Discussion

5.1 Paleoenvironmental implications of the proxy indices

5.1.1 TOC and TN contents, and C/N ratios

Organic matter in lake sediments has two principal sources, autochthonous (aquatic source) and allochthonous (terrestrial source), which are the plants living in the lake and its catchment, respectively (Talbot and Johannessen, 1992; Meyers, 1994). Algae and plankton are relatively protein-rich and cellulose-poor, and thus autochthonous organic matter has low atomic C/N ratios of between 4 and 10. In contrast, vascular land plants are commonly cellulose-rich but protein-poor, and hence exhibit high atomic C/N ratios of ≥20 (Meyers, 1994, 1997, 2003; Muller and Mathesius, 1999). Therefore, C/N ratios are extensively used to evaluate the relative contributions of terrestrial and aquatic organic matter to lake sediments (Meyers, 1990, 1994, 1997; Talbot and Johannessen, 1992; Meyers and Ishiwatari, 1993;

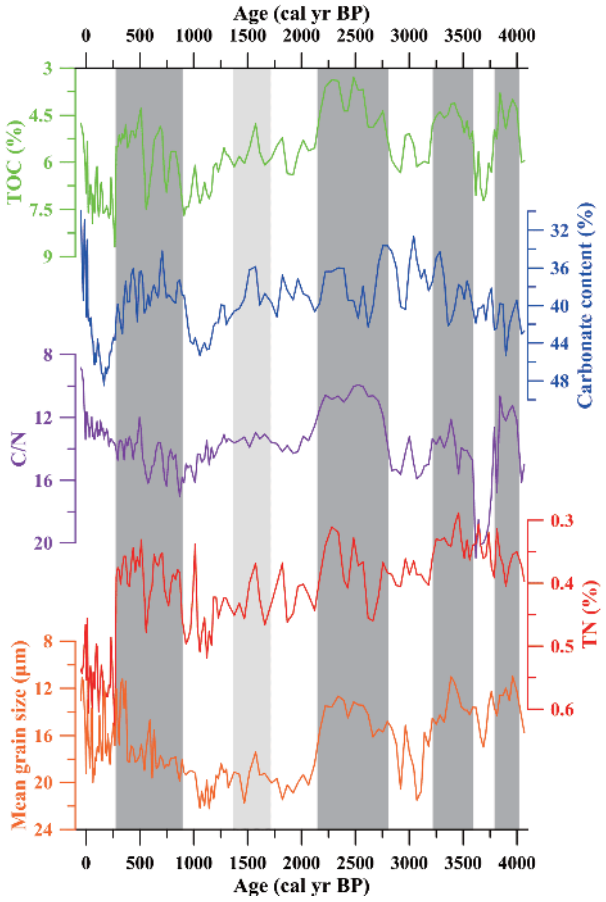

Figure 3 Multi-proxy indices in the SLM13-2-1 core. Gray bars highlight intervals of increased precipitation.

Meyers and Teranes, 2001; Lamb et al., 2006).

TOC and TN contents, and C/N ratios in lake sediments usually increase with higher primary production in the lake catchment, and result in a higher influx of TOC into the lake, in response to increased precipitation (Xiao et al., 2006; Xu et al., 2015). However, studies in Lake Sayram sediments region suggest that a higher flux of clastic sediments associated with increased precipitation would dilute TOC and TN contents, leading to lower TOC and TN. C/N ratios in Lake Sayram sediments should decrease with an increasing contribution from aquatic plants, resulting from the amelioration of the regional environment. Therefore, we interpret the TOC and TN contents, and C/N ratios of the Lake Sayram sediments to be proxy indices of regional precipitation changes, with decreasing TOC, TN, and C/N values reflecting increased precipitation, and vice versa.

5.1.2 Carbonate contents

In general, the rate of carbonate precipitation in a lake should be controlled predominantly by the ratio of evaporation to precipitation (E/P). Higher E/P results in carbonate supersaturation in lake water, and this may result in higher carbonate precipitation rates and higher carbonate contents in lake sediments. Previous studies have provided data that support the concept that carbonate contents in lake sediments reflect E/P (Chen F H et al., 2006; Xiao et al., 2006; Xu et al., 2006b, 2008; Wittkop et al., 2009). For example, a significant relationship between E/P values and carbonate contents has been reported for Lake Qinghai, China. Given that temperature is the primarily factor controlling evaporation at Lake Qinghai, the carbonate contents in Lake Qinghai sediments can be expected to be an indicator of regional temperature (Xu et al., 2006b, 2008). However, variations in lake sediment carbonate contents can be used as an indicator of regional effective moisture (Chen F H et al., 2006). For example, wet conditions have been identified from low carbonate contents in Lake Bosten and Lake Sasikul during the LIA (Chen F H et al., 2006; Lei et al., 2014).

Due to its location and hydrology, the formation of biogenic carbonate in Lake Sayram is limited. However, chemical carbonate precipitation results from extensive summer evaporation, and because the lake is usually ice covered usually from December to early May. Limestone is widely distributed in the Lake Sayram catchment (Wang, 1978) and the lake water has low Ca^{2+} and high HCO_3^- and CO_3^{2-} concentrations (Wang and Dou, 1998; Hu, 2004). As such, Ca^{2+} from runoff is effectively deposited with HCO_3^- and CO_3^{2-} to lake sediments, resulting in the high carbonate contents in Lake Sayram sediments. This is reflected in the high carbonate contents of the SLM13-2-1 core (average=~40.4%; Figure 3). With increased precipitation, the lower evaporation should lead to unsaturation of Ca^{2+} in lake water and greater transport of clastic sediments to the lake. Both these processes would dilute the carbonate contents in Lake Sayram sediments. Conversely, the carbonate contents should increase as precipitation decreases. Similar paleoenvironmental implications from carbonate contents have also been proposed for Lake Bosten (Chen F H et al., 2006; Zhang et al., 2010), Lake Dali (Xiao et al., 2008), and Lake Sasikul (Lei et al., 2014). Therefore, the carbonate contents of sediments in Lake Sayram can be used as an indicator of regional precipitation.

5.1.3 Grain size

Grain size of lake sediments directly or indirectly reflects the hydrodynamic conditions during the deposition, which is not only influenced by the lake features (e.g., area, size, shape, and topography), but also climate (mainly by precipitation) and vegetation changes in its catchment. Thus, grain size is widely used as an indicator of paleoclimate changes (Peng et al., 2005; Xiao et al., 2009, 2013, 2015; Xu et al., 2015; Lan et al., 2018). The mean grain size of lake sediments shows a concentric spatial distribution, with a coarser grain size in the littoral zone and finer grain size in the profundal zone. Lake Sayram is a medium-size but relatively deep lake and, as

such, coarser sediments are barely transported to the profundal zone. Therefore, the grain size of Lake Sayram sediments is predominantly fine- to medium-grained silt, with a mean grain size of 17 μm. Moreover, the area and water depth of Lake Sayram are variable (e.g., water depth increased by ~10 m in summer AD2016 as compared with summer AD2013). The hydrodynamic conditions at the sampling site would decrease, resulting from more profundal conditions, when the lake level increases due to increased precipitation. In turn, this would lead to finer-grained lake sediments. The decreasing mean grain size of uppermost sediments in the SLM13-2-1 core appears to reflect increased precipitation over the past several decades. Furthermore, studies of sediment grain size in Lake Daihai (Xiao et al., 2013) and Lake Dali (Xiao et al., 2015) have also identified decreased grain size linked to increased precipitation. Therefore, the mean grain size of the Lake Sayram sediments reflects regional precipitation changes.

5.2 Late Holocene hydroclimatic variations at Lake Sayram

Multi-proxy indices in the SLM13-2-1 core exhibit distinct and correlated temporal patterns during the past 4000 yr (Figure 3). Based on the above interpretations, these changes can potentially be used to reconstruct the past hydroclimatic variations at Lake Sayram (Figure 3). As shown in Figure 3, all the proxy indices have substantially lower values at 4000–3780, 3590–3210, 2800–2160, and 890–280 cal yr BP, which reveal four periods of increased precipitation. In addition, between 1700 and 1370 cal yr BP, a slightly decrease in the proxy indices implies a subtle increase in precipitation during the Dark Age Cold Period (DACP; Figure 3).

Furthermore, all the proxy indices show an unexpected decrease since ~100 cal yr BP, including the TOC contents (Figure 3), even though TOC contents commonly increase in surface lake sediments (Xiao et al., 2008; Xu et al., 2013; Anderson et al., 2014; Heathcote et al., 2015). These results suggest that human activity in the Lake Sayram region is negligible, and imply that all the proxy indices effectively record increasing precipitation at Lake Sayram region over the past 100 yr. This is in agreement with results from Lake Sayram published by Liu W et al. (2014) and also is all broadly comparable with instrumental records (Hu, 2004).

5.3 Hydroclimatic variations in mid-latitude Westerlies-dominated eastern Central Asia

When compared with regional paleoclimate records, the proxy indices in Lake Sayram provide insights into regional hydroclimatic variations at multi-decadal to centennial timescales, which are poorly documented in currently available climate reconstructions from eastern Central Asia. The spatial patterns of late Holocene hydroclimatic variations in this region are complex, due to apparently significant regional differences in past climate resulting from the interplay of different climatic systems (e.g., the mid-latitude Westerlies, the Siberian Anticyclone, and the Asian Summer Monsoon; Herzschuh, 2006; Chen et al., 2008, 2010; Rudaya et al., 2009; Wang W et al., 2013; Long et al., 2017; Wolff et al., 2017).

Hydroclimatic variations at Lake Sayram during the past 4000 cal yr BP are generally consistent with other records in eastern Central Asia (Figure 4), demonstrating similar patterns of late Holocene environmental and climate change. We verified the regional significance of our lake sediment profile as a precipitation-sensitive record by comparing the TOC data with a regional humidity record from Lake Kalakuli over the past 4000 years (Figure 4), inferred from leaf wax δD data (Aichner et al., 2015). TOC contents show a remarkable correspondence with δD isotope values. This confirms that TOC contents of the Lake Sayram sediments are a robust indicator of regional hydroclimatic variations. Due to dating uncertainties, sampling resolution, and site characteristics, the wet period at 3590–3210 cal yr BP is not documented in the Lake Kalakuli δD record, which might highlight the spatial complexity of late Holocene hydroclimate in eastern Central Asia.

However, similar to our record, speleothem δ^{18}O data from Uluu Cave (Wolff et al., 2017) and Kesang Cave (Cheng et al., 2012) record enhanced precipitation during this interval at a slightly different time. This broadly coincides with the pronounced increase in winter snowfall and meltwater supply during subsequent spring thaw in Central Kyrgyzstan (Lauterbach et al., 2014), higher lake levels at Lake Bosten, northwestern China (Mischke and Wunnemann, 2006), and humidity conditions at Lake Bangong, western Tibetan Plateau (Fontes et al., 1996). Moreover, generally lower pollen concentrations and minimum A/C ratios in Lake Manas coincide with higher TOC contents in Lake Sayram at ca. 3800–3600 cal yr BP, indicating a short periods of arid conditions during this interval (Rhodes et al., 1996). A previous study at Lake Sayram did not consider reservoir carbon effects on AMS^{14}C dating (Jiang et al., 2013) and does not match with our record. However, after correction for the reservoir carbon effect of 1073 yr, the A/C ratios reported by Jiang et al (2013) are also consistent with our records (Figure 4).

Over the past 2000 yr, our results have identified two periods of increased precipitation, with a significant increase in precipitation during the LIA (~890–280 cal yr BP) and a slightly increase in precipitation during the DACP (1700–1370 cal yr BP; Figure 4). This is broadly consistent with the hydroclimatic pattern documented throughout mid-latitude Westerlies-dominated Central Asia (Chen et al., 2010; Chen et al., 2015; Lan et al., 2018). Based on 17 paleo-hydrocli-

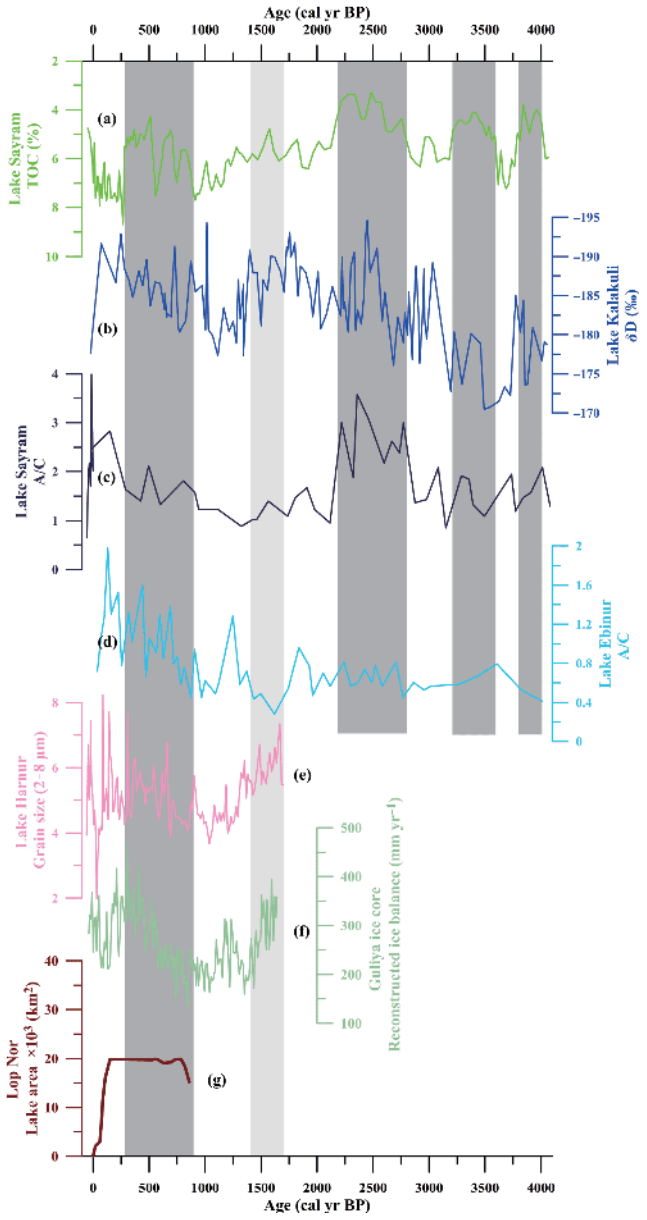

Figure 4 Comparison of hydroclimatic variations at Lake Sayram ((a), this study) with other records in mid-latitude Westerlies-dominated eastern Central Asia. (b) Lake Kalakuli (Aichner et al., 2015); (c) Lake Sayram (Jiang et al., 2013); (d) Lake Ebinur (Wang W et al., 2013); (e) Lake Harnur (Lan et al., 2018); (f) Guliya ice core (Yao et al., 1996; Thompson et al., 1997); (g) Lop Nor (Putnam et al., 2016).

matic records, Chen et al. (2010) proposed that wet LIA and dry MWP conditions existed in arid Central Asia over the past millennium, and suggested that this region was out-of-phase with conditions in monsoonal Asia. This was confirmed by a synthesis of hydroclimatic study in China and surrounding regions (Chen et al., 2015). Recently, Lan et al. (2018) suggested that similar warm-dry (MWP) and cold-wet (LIA) hydroclimatic patterns prevailed in high Central Aisa during the past two millennia. Pollen analysis from Lake Balkhash revealed increased precipitation between 650 and 100 cal yr BP (Feng et al., 2013). Arid MWP and humid LIA hydroclimatic conditions are also inferred from Lake Tiewaike in the Altai Mountains (Li et al., 2017) and Lake Manas in northwestern China (Song et al., 2015). Lake Ebinur in the Central Tianshan Mountains is close to our study site and had higher A/C ratios (Figure 4; Wang W et al., 2013), lower carbonate contents, and lighter organic matter and carbonate δ^{18}O values (Ma et al., 2011) during the LIA, in response to enhanced precipitation. Multi-proxy analysis, including carbonate contents, pollen assemblages, and grain size data of Lake Bosten revealed a humid climate during the LIA, and a warm-dry and cold-humid climate pattern on centennial timescales during the past 1000 yr (Chen F H et al., 2006). Negative carbon isotopic excursions of plant material from an aeolian sand profile in the arid eastern Tarim Basin also strongly indicate humid conditions during the LIA (Liu et al., 2011). δD values from Lake Son Kol in Central Kyrgyzstan record significantly increased summer moisture since 800 cal yr BP and decreased summer moisture between 1750 and 800 cal yr BP, which imply wet LIA and dry MWP climatic conditions (Lauterbach et al., 2014). More negatively δ^{18}O values for carbonate, and lower carbonate and sand contents in Lake Sasikul, Central Pamir, during the LIA record a wet period and higher lake level (Lei et al., 2014). Leaf wax δD values from Lake Kalakuli on the Pamir Plateau (Aichner et al., 2015) are relatively negative during the DACP and LIA (Figure 4), also indicating humid climate conditions during those intervals. Pollen record from the western margin of the Tarim Basin identified increased humidity condition at ~1750–1260 and ~550–390 cal yr BP (Zhao et al., 2012). Furthermore, an ice accumulation record for the Guliya ice core from the northern Tibetan Plateau (Figure 4; Yao et al., 1996; Thompson et al., 1997) revealed increased precipitation during the DACP and LIA, which is in agreement with other records from the mid-latitude Westerlies-dominated northern Tibetan Plateau (e.g., carbonate δ^{18}O in Lake Bangong, Fontes et al., 1996; pollen record in the Dunde ice core, Liu et al., 1998; tree ring δ^{18}O values from Delingha, Wang W Z et al., 2013).

Although the onset timing of the LIA in these previous studies is much younger than in our record (Figure 4), Putnam et al. (2016) showed that wetter LIA climate conditions characterized the core of the inner Asian desert belt at the beginning of early LIA in the late 1100s, which is closely consistent with our results (Figure 4). Therefore, increased precipitation likely occurred as early as 890 cal yr BP during the early LIA at Lake Sayram.

5.4 Possible forcing mechanisms for the late Holocene hydroclimatic variations in eastern Central Asia

The coherent late Holocene hydroclimatic patterns revealed by numerous studies in mid-latitude Westerlies-dominated

eastern Central Asia demonstrate that increased precipitation events were not a local signal, but were most likely a part of large synoptic-scale atmospheric circulation changes.

The inter-annual climate patterns in Central Asia are mainly controlled by the interplay between the mid-latitude Westerlies, the Siberia Anticyclone, and the Asian Summer Monsoon (Aizen et al., 1997, 2001, 2006; Chen et al., 2010; Cheng et al., 2012; Lauterbach et al., 2014; Wolff et al., 2017). However, as suggested by Cheng et al. (2012), Asian Summer Monsoon rainfall or related moisture can not penetrate into Central Asia during the times of low insolation, such as in the late Holocene. Furthermore, the lack of marine salts in snow at Muztag Ata (Pamir Plateau) supports the view that the Indian Summer Monsoon is only of minor importance source of the present-day precipitation (Seong et al., 2009). Although the Siberian High also appears to make only a minor contribution to annual precipitation, as it delivers cool and dry air, Wolff et al. (2017) suggested that it probably contributed significantly to climate variability at Uluu Cave in Central Asia. This is supported by Aizen et al. (2001), who suggested that precipitation is enhanced over the continental Asia when the Siberian High is positioned farther to the east than the west.

Based on firn/ice cores $\delta^{18}O$ data from the Altai (Belukha) and Tianshan mountains (Inilchek glacier), Aizen et al. (2006) concluded that precipitation in Central Asia is pre-

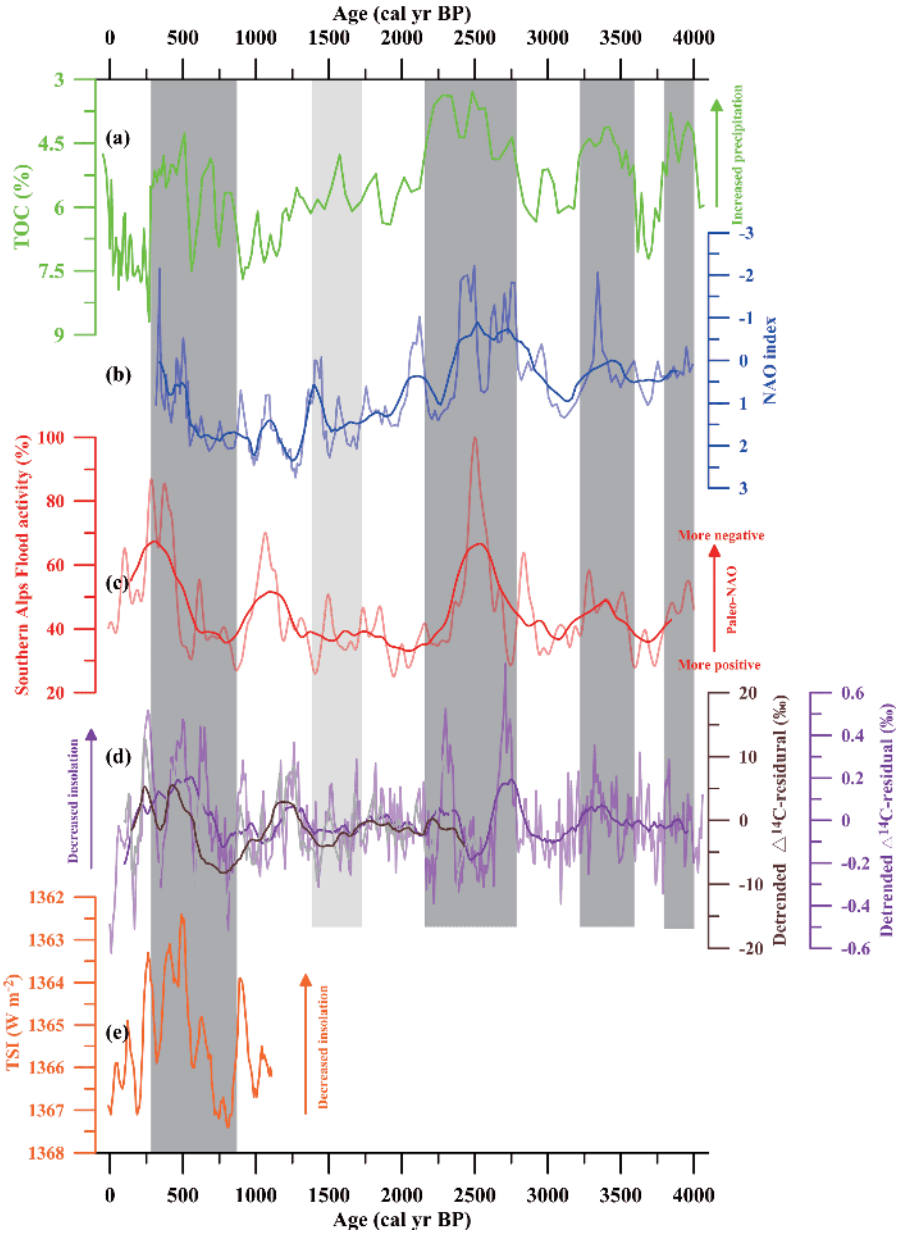

Figure 5 Comparison of the precipitation record from Lake Sayram ((a), this study) with a reconstruction of the NAO index ((b), Olsen et al., 2012), Southern Alps flood activity ((c), Wirth et al., 2013), de-trended $\triangle^{14}C$-residual ((d), Stuiver et al., 1998; Reimer et al., 2004), and total solar irradiance ((e), Bard et al., 2000).

dominantly regulated by the mid-latitude Westerlies transport of water vapor from the Aral-Caspian, Mediterranean, and Black Seas, and North Atlantic Ocean, which is consistent with modern air mass trajectories (Wolff et al., 2017). In addition, based on data from 145 meteorological stations, an inverse relationship between precipitation in Central Asia and the North Atlantic Oscillation Index (NAO) was shown by Aizen et al. (2001), who identified increased precipitation during the negative phase of the NAO and southward migration of the mid-latitude Westerlies. Using the KNMI Climate Explorer, Wolff et al. (2017) suggested that a more negative NAO triggered more precipitation in Central Asia from AD1950 to 2015. Comparison of our record with reconstructions of the NAO index from Greenland (Olsen et al., 2012), Southern Alps flood activity (a NAO index indicator; Wirth et al., 2013), and solar irradiance (Stuiver et al., 1998; Bard et al., 2000; Reimer et al., 2004) for the past 4000 years shows that increased precipitation periods in the Lake Sayram region are associated with a more negative NAO index, stronger Southern Alps flood activity, and lower solar irradiance (Figure 5). This highlights the influence of solar irradiance and southern migration of the entire circum-North Atlantic circulation system (Wirth et al., 2013), particularly the main pathway of the mid-latitude Westerlies, on Central Asia precipitation. This result agrees with earlier studies (Aizen et al., 2006; Chen et al., 2010; Lei et al., 2014; Lan et al., 2018; Wolff et al., 2017), which suggested that more southern displaced and wetter mid-latitude Westerlies occur during the negative NAO modes in Central Asia. For example, Chen et al. (2010) suggested that increased precipitation in arid Central Asia during the LIA could be attributed to the predominantly negative NAO index (Trouet et al., 2009) and, consequently, to enhanced moisture transport by the mid-latitude Westerlies responding to the high frequency of cyclonic activity in the North Atlantic and Mediterranean Ocean. Therefore, the underlying climatic factors and mechanisms of increased precipitation at Lake Sayram over the past 4000 yr are likely linked to the southward migration of the circum-North Atlantic circulation system (Trouet et al., 2009; Olsen et al., 2012; Wirth et al., 2013), which is possibly driven by lower solar irradiance (Stuiver et al., 1998; Bard et al., 2000; Reimer et al., 2004; Orme et al., 2017). However, the mechanisms that ultimately force the mid-latitude Westerlies require further investigation (Deininger et al., 2017).

6. Conclusions

In this study, we used a high-resolution lake sediment record from the Central Tianshan Mountains (Lake Sayram) to reconstruct regional hydroclimatic variations at multi-decadal to centennial timescales, and to investigate possible late Holocene climate forcing mechanisms. Our results reveal five periods of increased precipitation periods at 4000–3780, 3590–3210, 2800–2160, 1700–1370, and 890–280 cal yr BP in the Lake Sayram region, which are broadly consistent with other paleo-records from the eastern Central Asia. This indicates that coherent regional hydroclimatic changes occurred during the late Holocene in mid-latitude Westerlies-dominated eastern Central Asia. A close correspondence between our record and reconstructions of the NAO index and solar irradiance suggests that decreasing solar irradiance and southward migration of the entire circum-North Atlantic circulation system, particularly the main pathway of the mid-latitude Westerlies, significantly influence eastern Central Asia hydroclimate. In addition, precipitation appears to have increased over the past 100 yr, although possible future hydroclimatic changes require further investigation.

Acknowledgements *This work is a part of The "Belt & Road" Project of the Institute of Earth and Environment, Chinese Academy of Sciences. This work was supported by the National Natural Science Foundation of China (Grant Nos. 41672169, 41473120 & 41502171) and the Youth Innovation Promotion Association of Chinese Academy of Sciences (Grant No. 2012295).*

References

Aichner B, Feakins S J, Lee J E, Herzschuh U, Liu X. 2015. High-resolution leaf wax carbon and hydrogen isotopic record of the late Holocene paleoclimate in arid Central Asia. Clim Past, 11: 619–633

Aizen E M, Aizen V B, Melack J M, Nakamura T, Ohta T. 2001. Precipitation and atmospheric circulation patterns at mid-latitudes of Asia. Int J Climatol, 21: 535–556

Aizen V B, Aizen E M, Joswiak D R, Fujita K, Takeuchi N, Nikitin S A. 2006. Climatic and atmospheric circulation pattern variability from ice-core isotope/geochemistry records (Altai, Tien Shan and Tibet). Ann Glaciol, 43: 49–60

Aizen V B, Aizen E M, Melack J M, Dozier J. 1997. Climatic and hydrologic changes in the Tien Shan, Central Asia. J Clim, 10: 1393–1404

Anderson N J, Bennion H, Lotter A F. 2014. Lake eutrophication and its implications for organic carbon sequestration in Europe. Glob Change Biol, 20: 2741–2751

Appleby P G. 2001. Chronostratigraphic techniques in recent sediments. In: Last W M, Smol J P, eds. Tracking Environmental Change Using Lake Sediments: Basin Analysis, Coring, and Chronological Techniques. Dordrecht: Springer Netherlands. 171–203

Appleby P G, Oldfield F, Thompson R, Huttunen P, Tolonen K. 1979. ^{210}Pb dating of annually laminated lake sediments from Finland. Nature, 280: 53–55

Bard E, Raisbeck G, Yiou F, Jouzel J. 2000. Solar irradiance during the last 1200 years based on cosmogenic nuclides. Tellus B-Chem Phys Meteorol, 52: 985–992

Bond G, Kromer B, Beer J, Muscheler R, Evans M N, Showers W, Hoffmann S, Lotti-Bond R, Hajdas I, Bonani G. 2001. Persistent solar influence on North Atlantic climate during the Holocene. Science, 294: 2130–2136

Buckley B M, Anchukaitis K J, Penny D, Fletcher R, Cook E R, Sano M, Canh Nam L, Wichienkeeo A, That Minh T, Hong T M. 2010. Climate as a contributing factor in the demise of Angkor, Cambodia. Proc Natl Acad Sci USA, 107: 6748–6752

Chen F H, Chen J H, Holmes J, Boomer I, Austin P, Gates J B, Wang N L,

Brooks S J, Zhang J W. 2010. Moisture changes over the last millennium in arid central Asia: A review, synthesis and comparison with monsoon region. Quat Sci Rev, 29: 1055–1068
Chen F H, Huang X Z, Zhang J W, Holmes J A, Chen J H. 2006. Humid little ice age in arid central Asia documented by Bosten Lake, Xinjiang, China. Sci China Ser-Earth Sci, 49: 1280–1290
Chen F H, Yu Z C, Yang M L, Huang X, Zhao Y, Sato T, Birks H J B, Boomer I, Chena J, Ana C, Wunnemannj B. 2008. Holocene moisture evolution in arid central Asia and its out-of-phase relationship with Asian monsoon history. Quat Sci Rev, 27: 351–364
Chen J H, Chen F H, Feng S, Huang W, Liu J B, Zhou A F. 2015. Hydroclimatic changes in China and surroundings during the Medieval climate anomaly and little ice age: Spatial patterns and possible mechanisms. Quat Sci Rev, 107: 98–111
Chen Y N, Li W H, DengH J, Fang G H, Li Z. 2016. Changes in central Asia's water tower: Past, present and future. Sci Rep, 6: 35458
Cheng H, Zhang P Z, Spötl C, Edwards R L, Cai Y J, Zhang D Z, Sang W C, Tan M, An Z S. 2012. The climatic cyclicity in semiarid-arid central Asia over the past 500000 years. Geophys Res Lett, 39: L01705
Cook E R, Woodhouse C A, Eakin C M, Meko D M, Stahle D W. 2004. Long-term aridity changes in the western United States. Science, 306: 1015–1018
Deininger M, McDermott F, Mudelsee M, Werner M, Frank N, Mangini A. 2017. Coherency of late Holocene European speleothem δ^{18}O records linked to North Atlantic Ocean circulation. Clim Dyn, 49: 595–618
Diaz H F, Trigo R, Hughes M K, Mann M E, Xoplaki E, Barriopedro D. 2011. Spatial and temporal characteristics of climate in Medieval Times revisited. Bull Amer Meteorol Soc, 92: 1487–1500
Feng Z D, Wu H N, Zhang C J, Ran M, Sun A Z. 2013. Bioclimatic change of the past 2500 years within the Balkhash Basin, eastern Kazakhstan, Central Asia. Quat Int, 311: 63–70
Fontes J C, Gasse F, Gibert E. 1996. Holocene environmental changes in Lake Bangong basin (western Tibet). Part 1: Chronology and stable isotopes of carbonates of a Holocene lacustrine core. Palaeogeogr Palaeoclimatol Palaeoecol, 120: 25–47
Graham N E, Ammann C M, Fleitmann D, Cobb K M, Luterbacher J. 2011. Support for global climate reorganization during the "Medieval Climate Anomaly". Clim Dyn, 37: 1217–1245
Gray L J, Beer J, Geller M, Haigh J D, Lockwood M, Matthes K, Cubasch U, Fleitmann D, Harrison G, Hood L, Luterbacher J, Meehl G A, Shindell D, van Geel B, White W. 2010. Solar influences on climate. Rev Geophys, 48: RG4001
Heathcote A J, Anderson N J, Prairie Y T, Engstrom D R, del Giorgio P A. 2015. Large increases in carbon burial in northern lakes during the Anthropocene. Nat Commun, 6: 10016
Herzschuh U. 2006. Palaeo-moisture evolution in monsoonal Central Asia during the last 50000 years. Quat Sci Rev, 25: 163–178
Hodell D A, Brenner M, Curtis J H, Guilderson T. 2001. Solar forcing of drought frequency in the Maya lowlands. Science, 292: 1367–1370
Hodell D A, Curtis J H, Brenner M. 1995. Possible role of climate in the collapse of Classic Maya civilization. Nature, 375: 391–394
Hou J Z, D'Andrea W J, Liu Z H. 2012. The influence of ^{14}C reservoir age on interpretation of paleolimnological records from the Tibetan Plateau. Quat Sci Rev, 48: 67–79
Hu R J. 2004. Physical Geography of the Tianshan Mountaions in China (in Chinese). Beijing: China Environmental Science Press. 278–284
Huang X T, Oberhansli H, von S H, Prasad S, Sorrel P, Plessen B, Mathis M, Usubaliev R. 2014. Hydrological changes in western Central Asia (Kyrgyzstan) during the Holocene as inferred from a palaeolimnological study in lake Son Kul. Quat Sci Rev, 103: 134–152
IPCC. 2007. Climate Change 2007: The Physical Science Basis. Cambridge: Cambridge University Press. 996
Jiang Q F, Ji J F, Shen J, Matsumoto R, Tong G B, Qian P, Ren X M, Yan D Z. 2013. Holocene vegetational and climatic variation in westerly-dominated areas of Central Asia inferred from the Sayram Lake in northern Xinjiang, China. Sci China Earth Sci, 56: 339–353
Klaminder J, Appleby P, Crook P, Renberg I. 2012. Post-deposition diffusion of ^{137}Cs in lake sediment: Implications for radiocaesium dating. Sedimentology, 59: 2259–2267
Lamb A L, Wilson G P, Leng M J. 2006. A review of coastal palaeoclimate and relative sea-level reconstructions using δ^{13}C and C/N ratios in organic material. Earth-Sci Rev, 75: 29–57
Lan J H, Xu H, Sheng E G, Yu K K, Wu H X, Zhou K E, Yan D N, Ye Y D, Wang T L. 2018. Climate changes reconstructed from a glacial lake in High Central Asia over the past two millennia. Quat Int, 487: 43–53
Lauterbach S, Witt R, Plessen B, Dulski P, Prasad S, Mingram J, Gleixner G, Hettler-Riedel S, Stebich M, Schnetger B, Schwalb A, Schwarz A. 2014. Climatic imprint of the mid-latitude Westerlies in the Central Tian Shan of Kyrgyzstan and teleconnections to North Atlantic climate variability during the last 6000 years. Holocene, 24: 970–984
Lei Y B, Tian L D, Bird B W, Hou J Z, Ding L, Oimahmadov I, Gadoev M. 2014. A 2540-year record of moisture variations derived from lacustrine sediment (Sasikul Lake) on the Pamir Plateau. Holocene, 24: 761–770
Li X Q, Zhao K L, Dodson J, Zhou X Y. 2011. Moisture dynamics in central Asia for the last 15 kyr: New evidence from Yili Valley, Xinjiang, NW China. Quat Sci Rev, 30: 3457–3466
Li Y, Qiang M R, Zhang J W, Huang X Z, Zhou A F, Chen J H, Wang G G, Zhao Y. 2017. Hydroclimatic changes over the past 900 years documented by the sediments of Tiewaike Lake, Altai Mountains, Northwestern China. Quat Int, 452: 91–101
Liu K, Yao Z, Thompson L G. 1998. A pollen record of Holocene climatic changes from the Dunde ice cap, Qinghai-Tibetan Plateau. Geology, 26: 135
Liu W, Wu J, Ma L, Zeng H. 2014. A 200-year sediment record of environmental change from Lake Sayram, Tianshan Mountains in China. GFF, 136: 548–555
Liu W, Wu J L, Ma L, Zeng H A. 2011. Wet climate during the 'Little Ice Age' in the arid Tarim Basin, northwestern China. Holocene, 21: 409–416
Liu X Q, Dong H L, Yang X D, Herzschuh U, Zhang E L, Stuut J B W, Wang Y B. 2009. Late Holocene forcing of the Asian winter and summer monsoon as evidenced by proxy records from the northern Qinghai-Tibetan Plateau. Earth Planet Sci Lett, 280: 276–284
Liu X Q, Herzschuh U, Wang Y B, Kuhn G, Yu Z T. 2014. Glacier fluctuations of Muztagh Ata and temperature changes during the late Holocene in westernmost Tibetan Plateau, based on glaciolacustrine sediment records. Geophys Res Lett, 41: 6265–6273
Liu Y, An Z S, Linderholm H W, Chen D L, Song H M, Cai Q F, Sun J Y, Tian H. 2009. Annual temperatures during the last 2485 years in the mid-eastern Tibetan Plateau inferred from tree rings. Sci China Ser D-Earth Sci, 52: 348–359
Long H, Shen J, Chen J, Tsukamoto S, Yang L, Cheng H, Frechen M. 2017. Holocene moisture variations over the arid central Asia revealed by a comprehensive sand-dune record from the central Tian Shan, NW China. Quat Sci Rev, 174: 13–32
Ma L, Wu J, Yu H, Haiao Z, Abuduwaili J. 2011. The medieval warm period and the little ice age from a sediment record of Lake Ebinur, northwest China. Boreas, 40: 518–524
Meyers P A. 1990. Impacts of late Quaternary fluctuations in water level on the accumulation of sedimentary organic matter in Walker Lake, Nevada. Palaeogeogr Palaeoclimatol Palaeoecol, 78: 229–240
Meyers P A. 1994. Preservation of elemental and isotopic source identification of sedimentary organic matter. Chem Geol, 114: 289–302
Meyers P A. 1997. Organic geochemical proxies of paleoceanographic, paleolimnologic, and paleoclimatic processes. Org Geochem, 27: 213–250
Meyers P A. 2003. Applications of organic geochemistry to paleolimnological reconstructions: A summary of examples from the Laurentian Great Lakes. Org Geochem, 34: 261–289
Meyers P A, Ishiwatari R. 1993. Lacustrine organic geochemistry—An overview of indicators of organic matter sources and diagenesis in lake sediments. Org Geochem, 20: 867–900
Meyers P A, Teranes J L. 2001. Sediment organic matter. In: Last W M, Smol J P, eds. Tracking Environmental Change Using Lake Sediments.

Volume 2: Physical and Geochemical Methods. Netherlands: Kluwer Academic Publishers. 239–240
Mischke S, Wunnemann B. 2006. The Holocene salinity history of Bosten Lake (Xinjiang, China) inferred from ostracod species assemblages and shell chemistry: Possible palaeoclimatic implications. Quat Int, 154-155: 100–112
Moffa-Sánchez P, Born A, Hall I R, Thornalley D J R, Barker S. 2014. Solar forcing of North Atlantic surface temperature and salinity over the past millennium. Nat Geosci, 7: 275–278
Muller A, Mathesius U. 1999. The palaeoenvironments of coastal lagoons in the southern Baltic Sea, I. The application of sedimentary C-org/N ratios as source indicators of organic matter. Palaeogeogr Palaeoclim Palaeoeco, 145: 1–16
Olsen J, Anderson N J, Knudsen M F. 2012. Variability of the North Atlantic oscillation over the past 5200 years. Nat Geosci, 5: 808–812
Orme L C, Charman D J, Reinhardt L, Jones R T, Mitchell F J G, Stefanini B S, Barkwith A, Ellis M A, Grosvenor M. 2017. Past changes in the North Atlantic storm track driven by insolation and sea-ice forcing. Geology, 45: 335–338
Pederson N, Hessl A E, Baatarbileg N, Anchukaitis K J, Di Cosmo N. 2014. Pluvials, droughts, the Mongol Empire, and modern Mongolia. Proc Natl Acad Sci USA, 111: 4375–4379
Peng Y J, Xiao J, Nakamura T, Liu B L, Inouchi Y. 2005. Holocene East Asian monsoonal precipitation pattern revealed by grain-size distribution of core sediments of Daihai Lake in Inner Mongolia of north-central China. Earth Planet Sci Lett, 233: 467–479
Pennington W, Tutin T G, Cambray R S, Fisher E M. 1973. Observations on lake sediments using fallout ^{137}Cs as a tracer. Nature, 242: 324–326
Putnam A E, Putnam D E, Andreu-Hayles L, Cook E R, Palmer J G, Clark E H, Wang C, Chen F, Denton G H, Boyle D P, Bassett S D, Birkel S D, Martin-Fernandez J, Hajdas I, Southon J, Garner C B, Cheng H, Broecker W S. 2016. Little Ice Age wetting of interior Asian deserts and the rise of the Mongol Empire. Quat Sci Rev, 131: 33–50
Putyrskaya V, Klemt E, Röllin S. 2009. Migration of ^{137}Cs in tributaries, lake water and sediment of Lago Maggiore (Italy, Switzerland)—Analysis and comparison with Lago di Lugano and other lakes. J Environ Radioact, 100: 35–48
Reimer P J, Baillie M G L, Bard E, Bayliss A, Warren Beck J, Bertrand C J H, Blackwell P G, Buck C E, Burr G S, Cutler K B, Damon P E, Lawrence Edwards R, Fairbanks R G, Friedrich M, Guilderson T P, Hogg A G, Hughen K A, Kromer B, McAffmac G, Manning S, Bronk Ramsey C, Reimer R W, Remmele S, Southon J R, Stuiver M, Talamo S, Taylor F W, van der Plicht J, Weyhenmeyer C E. 2004. Intcal04 terrestrial radiocarbon age calibration, 0–26 cal kyr BP. Radiocarbon, 46: 1029–1058
Reimer P J, Baillie M G L, Bard E, Bayliss A, Beck J W, Blackwell P G, Bronk Ramsey C, Buck C E, Burr G S, Edwards R L, Friedrich M, Grootes P M, Guilderson T P, Hajdas I, Heaton T J, Hogg A G, Hughen K A, Kaiser K F, Kromer B, McCormac F G, Manning S W, Reimer R W, Richards D A, Southon J R, Talamo S, Turney C S M, van der Plicht J, Weyhenmeyer C E. 2009. Intcal09 and marine09 radiocarbon age calibration curves, 0–50000 years cal BP. Radiocarbon, 51: 1111–1150
Rhodes T E, Gasse F, Lin R, Fontes J C, Wei K, Bertrand P, Gibert E, Mélières F, Tucholka P, Wang Z, Cheng Z Y. 1996. A late Pleistocene-Holocene lacustrine record from Lake Manas, Zunggar (northern Xinjiang, western China). Palaeogeogr Palaeoclimatol Palaeoecol, 120: 105–121
Robbins J A, Edgington D N. 1975. Determination of recent sedimentation rates in Lake Michigan using Pb-210 and Cs-137. Geochim Cosmochim Acta, 39: 285–304
Rudaya N, Tarasov P, Dorofeyuk N, Solovieva N, Kalugin I, Andreev A, Daryin A, Diekmann B, Riedel F, Tserendash N, Wagner M. 2009. Holocene environments and climate in the Mongolian Altai reconstructed from the Hoton-Nur pollen and diatom records: A step towards better understanding climate dynamics in Central Asia. Quat Sci Rev, 28: 540–554
Sanchez-Cabeza J A, Ruiz-Fernández A C. 2012. ^{210}Pb sediment radiochronology: An integrated formulation and classification of dating models. Geochim Cosmochim Acta, 82: 183–200
Schurer A P, Tett S F B, Hegerl G C. 2014. Small influence of solar variability on climate over the past millennium. Nat Geosci, 7: 104–108
Seong Y B, Owen L A, Yi C, Finkel R C, Schoenbohm L. 2009. Geomorphology of anomalously high glaciated mountains at the northwestern end of Tibet: Muztag Ata and Kongur Shan. Geomorphology, 103: 227–250
Sha L, Jiang H, Seidenkrantz M S, Knudsen K L, Olsen J, Kuijpers A, Liu Y. 2014. A diatom-based sea-ice reconstruction for the Vaigat Strait (Disko Bugt, West Greenland) over the last 5000 yr. Palaeogeogr Palaeoclimatol Palaeoecol, 403: 66–79
Sha L, Jiang H, Seidenkrantz M S, Muscheler R, Zhang X, Knudsen M F, Olsen J, Knudsen K L, Zhang W. 2016. Solar forcing as an important trigger for West Greenland sea-ice variability over the last millennium. Quat Sci Rev, 131: 148–156
Sigl M, Winstrup M, McConnell J R, Welten K C, Plunkett G, Ludlow F, Büntgen U, Caffee M, Chellman N, Dahl-Jensen D, Fischer H, Kipfstuhl S, Kostick C, Maselli O J, Mekhaldi F, Mulvaney R, Muscheler R, Pasteris D R, Pilcher J R, Salzer M, Schüpbach S, Steffensen J P, Vinther B M, Woodruff T E. 2015. Timing and climate forcing of volcanic eruptions for the past 2500 years. Nature, 523: 543–549
Song M, Zhou A F, Zhang X N, Zhao C, He Y X, Yang W Q, Liu W G, Li S H, Liu Z H. 2015. Solar imprints on Asian inland moisture fluctuations over the last millennium. Holocene, 25: 1935–1943
Stuiver M, Reimer P J. 1993. Extended ^{14}C data base and revised calib 3.0 ^{14}C age calibration program. Radiocarbon, 35: 215–230
Stuiver M, Reimer P J, Bard E, Beck J W, Burr G S, Hughen K A, Kromer B, McCormac G, Van Der Plicht J, Spurk M. 1998. Intcal98 radiocarbon age calibration, 24000–0 cal BP. Radiocarbon, 40: 1041–1083
Sun Y B, Clemens S C, Morrill C, Lin X P, Wang X L, An Z S. 2011. Influence of Atlantic meridional overturning circulation on the East Asian winter monsoon. Nat Geosci, 5: 46–49
Sun Y B, Kutzbach J, An Z S, Clemens S, Liu Z Y, Liu W G, Liu X D, Shi Z G, Zheng W P, Liang L J, Yan Y, Li Y. 2015. Astronomical and glacial forcing of East Asian summer monsoon variability. Quat Sci Rev, 115: 132–142
Swingedouw D, Terray L, Cassou C, Voldoire A, Salas-Mélia D, Servonnat J. 2011. Natural forcing of climate during the last millennium: Fingerprint of solar variability. Clim Dyn, 36: 1349–1364
Talbot M R, Johannessen T. 1992. A high resolution palaeoclimatic record for the last 27500 years in tropical West Africa from the carbon and nitrogen isotopic composition of lacustrine organic matter. Earth Planet Sci Lett, 110: 23–37
Tan L C, Cai Y J, An Z S, Cheng H, Shen C C, Breitenbach S F M, Gao Y L, Edwards R L, Zhang H W, Du Y J. 2015. A Chinese cave links climate change, social impacts, and human adaptation over the last 500 years. Sci Rep, 5: 12284
Thiéblemont R, Matthes K, Omrani N E, Kodera K, Hansen F. 2015. Solar forcing synchronizes decadal North Atlantic climate variability. Nat Commun, 6: 8268
Thompson L G, Yao T, Davis M E, Henderson K A, MosleyThompson E, Lin P N, Beer J, Synal H A, ColeDai J, Bolzan J F. 1997. Tropical climate instability: The last glacial cycle from a Qinghai-Tibetan ice core. Science, 276: 1821–1825
Trouet V, Esper J, Graham N E, Baker A, Scourse J D, Frank D C. 2009. Persistent positive North Atlantic oscillation mode dominated the medieval climate anomaly. Science, 324: 78–80
Wan G J. 1995. Progresses on ^{137}Cs and ^{210}Pb$_{ex}$ dating of lake sediments (in Chinese). Adv Earth Sci, 10: 188–192
Wang S J. 1978. The relationship between formation and evolution of Lake Sayram and glacier activity during the Quaternary (in Chinese). Arid Land Geogr, 1: 47–55
Wang S M, Dou H S. 1998. China Lakes Record (in Chinese). Beijing: Science Press. 348–349
Wang W Z, Liu X H, Xu G B, Shao X M, Qin D H, Sun W Z, An W L, Zeng X M. 2013. Moisture variations over the past millennium char-

acterized by Qaidam Basin tree-ring δ^{18}O. Chin Sci Bull, 58: 3956–3961
Wang W, Feng Z D, Ran M, Zhang C J. 2013. Holocene climate and vegetation changes inferred from pollen records of Lake Aibi, northern Xinjiang, China: A potential contribution to understanding of Holocene climate pattern in East-central Asia. Quat Int, 311: 54–62
Wieland E, Santschi P H, Höhener P, Sturm M. 1993. Scavenging of chernobyl ^{137}Cs and natural ^{210}Pb in Lake Sempach, Switzerland. Geochim Cosmochim Acta, 57: 2959–2979
Wirth S B, Glur L, Gilli A, Anselmetti F S. 2013. Holocene flood frequency across the Central Alps-solar forcing and evidence for variations in North Atlantic atmospheric circulation. Quat Sci Rev, 80: 112–128
Wittkop C A, Teranes J L, Dean W E, Guilderson T P. 2009. A lacustrine carbonate record of Holocene seasonality and climate. Geology, 37: 695–698
Wolff C, Plessen B, Dudashvilli A S, Breitenbach S F, Cheng H, Edwards L R, Strecker M R. 2017. Precipitation evolution of Central Asia during the last 5000 years. Holocene, 27: 142–154
Wu J L, Zeng H A, Ma L, Bai R D. 2012. Recent changes of selected lake water resoures in arid Xinjiang, Northwestern China (in Chinese). Quat Sci, 32: 142–150
Xiao J L, Fan J W, Zhai D Y, Wen R L, Qin X G. 2015. Testing the model for linking grain-size component to lake level status of modern clastic lakes. Quat Int, 355: 34–43
Xiao J L, Fan J W, Zhou L, Zhai D Y, Wen R L, Qin X G. 2013. A model for linking grain-size component to lake level status of a modern clastic lake. J Asian Earth Sci, 69: 149–158
Xiao J L, Chang Z, Si B, Qin X, Itoh S, Lomtatidze Z. 2009. Partitioning of the grain-size components of Dali Lake core sediments: Evidence for lake-level changes during the Holocene. J Paleolimnol, 42: 249–260
Xiao J L, Si B, Zhai D Y, Itoh S, Lomtatidze Z. 2008. Hydrology of Dali Lake in central-eastern Inner Mongolia and Holocene East Asian monsoon variability. J Paleolimnol, 40: 519–528
Xiao J L, Wu J, Si B, Liang W, Nakamura T, Liu B, Inouchi Y. 2006. Holocene climate changes in the monsoon/arid transition reflected by carbon concentration in Daihai Lake of Inner Mongolia. Holocene, 16: 551–560
Xu H, Ai L, Tan L, An Z. 2006a. Geochronology of a surface core in the northern basin of Lake Qinghai: Evidence from ^{210}Pb and ^{137}Cs radionuclides. Chin J Geochem, 25: 301–306
Xu H, Ai L, Tan L, An Z. 2006b. Stable isotopes in bulk carbonates and organic matter in recent sediments of Lake Qinghai and their climatic implications. Chem Geol, 235: 262–275
Xu H, Lan J, Liu B, Sheng E, Yeager K M. 2013. Modern carbon burial in Lake Qinghai, China. Appl Geochem, 39: 150–155
Xu H, Liu X Y, An Z S, Hou Z H, Dong J B, Liu B. 2010. Spatial pattern of modern sedimentation rate of Qinghai Lake and a preliminary estimate of the sediment flux. Chin Sci Bull, 55: 621–627
Xu H, Liu X, Hou Z. 2008. Temperature variations at Lake Qinghai on decadal scales and the possible relation to solar activities. J Atmos Sol-Terr Phys, 70: 138–144
Xu H, Zhou X Y, Lan J H, Liu B, Sheng E G, Yu K K, Cheng P, Wu F, Hong B, Yeager K M, Xu S. 2015. Late Holocene Indian summer monsoon variations recorded at Lake Erhai, Southwestern China. Quat Res, 83: 307–314
Yan H, Sun L, Wang Y, Huang W, Qiu S, Yang C. 2011. A record of the Southern Oscillation Index for the past 2000 years from precipitation proxies. Nat Geosci, 4: 611–614
Yan H, Wei W, Soon W, An Z, Zhou W, Liu Z, Wang Y, Carter R M. 2015. Dynamics of the intertropical convergence zone over the western Pacific during the Little Ice Age. Nat Geosci, 8: 315–320
Yang B, Wang J, Brauning A, Dong Z, Esper J. 2009. Late Holocene climatic and environmental changes in arid central Asia. Quat Int, 194: 68–78
Yao T D, Qin D H, Tian L D, Jiao K Q, Yang Z H, Xie C, Thompson L G. 1996. Variations in temperature and precipitation in the past 2000 a on the Xizang (Tibet) Plateau——Guliya ice core record. Sci China Ser D-Earth Sci, 39: 425–433
Yu K, Xu H, Lan J, Sheng E, Liu B, Wu H, Tan L, Yeager K M. 2017. Climate change and soil erosion in a small alpine lake basin on the Loess Plateau, China. Earth Surf Process Land, 42: 1238–1247
Yu S Y, Cheng P, Hou Z F. 2014. A caveat on radiocarbon dating of organic-poor bulk lacustrine sediments in arid China. Radiocarbon, 56: 127–141
Zhang C, Feng Z, Yang Q, Gou X, Sun F. 2010. Holocene environmental variations recorded by organic-related and carbonate-related proxies of the lacustrine sediments from Bosten Lake, northwestern China. Holocene, 20: 363–373
Zhang P Z, Cheng H, Edwards R L, Chen F H, Wang Y J, Yang X L, Liu J, Tan M, Wang X F, Liu J H, An C L, Dai Z B, Zhou J, Zhang D Z, Jia J H, Jin L Y, Johnson K R. 2008. A test of climate, sun, and culture relationships from an 1810-year Chinese cave record. Science, 322: 940–942
Zhao K L, Li X Q, Dodson J, Atahan P, Zhou X Y, Bertuch F. 2012. Climatic variations over the last 4000 cal yr BP in the western margin of the Tarim Basin, Xinjiang, reconstructed from pollen data. Palaeogeogr Palaeoclimatol Palaeoecol, 321-322: 16–23

(Responsible editor: Jule XIAO)